Materials Transactions, Vol. 53, No. 11 (2012) pp. 1992 to 1996

Conversion Kinetics of Cerium Oxide into Sodium Cerium Sulfate in Na_2SO_4–H_2SO_4–H_2O Solutions

Namil Um and Tetsuji Hirato*

Department of Energy Science and Technology, Graduate School of Energy Science, Kyoto University, Kyoto 611-0011, Japan

The conversion of cerium oxide (CeO_2) into sodium cerium sulfate ($NaCe(SO_4)_2{\cdot}H_2O$) in Na_2SO_4–H_2SO_4–H_2O solutions was studied at elevated temperatures using a batch-type glass reactor under atmospheric pressure. Sodium sulfate (Na_2SO_4) concentration, sulfuric acid (H_2SO_4) concentration and reaction temperature were chosen as dependent variables, and the effects of these three variables on the conversion of cerium oxide into sodium cerium sulfate in Na_2SO_4–H_2SO_4–H_2O solutions were investigated. The conversion includes two chemical reactions: cerium oxide dissolution and sodium cerium sulfate synthesis. The experimental data showed that increases of sodium sulfate concentration and sulfuric acid concentration decreased the conversion rate, whereas the conversion rate increased with increasing reaction temperature. The conversion kinetics of cerium oxide into sodium cerium sulfate for these three variables was analyzed and the fitted equation to the experimental data was determined. The variations of rate constant in dissolution and synthesis with temperature obeyed the Arrhenius equation with activation energies of 120 and 200 kJ/mol, respectively. In addition, the rate constant of cerium oxide dissolution was a function of the sodium sulfate concentration and sulfuric acid concentration at $N^{-0.3}$ and $C^{6.5}$, respectively, and for sodium cerium oxide synthesis at $N^{-0.2}$ and $C^{-4.3}$.
[doi:10.2320/matertrans.M-M2012827]

(Received August 1, 2012; Accepted August 25, 2012; Published October 11, 2012)

Keywords: *cerium oxide, sodium cerium sulfate, sulfuric acid, conversion kinetics, shrinking-core model*

1. Introduction

The use of rare earth polishing powder has achieved improvements in the efficiency of the industrial polishing process since engineers who were processing optical glass began to use polishing powder made from rare earth elements, especially cerium oxide, which can be used for highly productive polishing powder.[1–4] These powders have become the best materials for the polishing process. Since rare earth metal is widely used as a polishing powder for glass, semiconductors, and ceramics, large amounts of polishing powder waste containing rare earth metals have been generated.[5] Unfortunately, most of the rare earth polishing powder waste (REPPW) has been buried in landfill because it is not easy to treat chemically or physically. In addition, there is also increasing demand for rare earth metals in various fields besides their application in rare earth polishing powder. Therefore, many researchers are beginning to take interest in the recovery of rare earth metals from REPPW by a hydrometallurgical method including ion exchange, solvent extraction, electrolysis, and leaching.[6–9]

The leaching process can be employed for cerium recovery from REPPW. However, cerium oxide is the most stable phase at room temperature and under atmospheric conditions, and so its dissolution in acid solutions has many difficulties. Even if cerium oxide is ionized by acid solutions, there is also difficulty in purifying it from polished objects containing non rare earth metal ions (Al^{3+}, Ca^{2+}, etc.). Usually, for purification, the rare earth elements are precipitated in the form of rare earths and sodium double sulfate ($NaRE(SO_4)_2{\cdot}xH_2O$) through the addition of sodium sulfate.[10] If cerium oxide, therefore, is converted into sodium cerium sulfate in Na_2SO_4–H_2SO_4–H_2O solutions during the leaching-REPPW process, it would be one of the simpler separation methods because sodium cerium sulfate is poorly soluble under acidic conditions.[11] This simple method, aimed at sodium cerium sulfate ($NaCe(SO_4)_2{\cdot}H_2O$), has been applied in various fields.[12–14]

Therefore, the aim of this study was to investigate the conversion kinetics of cerium oxide into sodium cerium sulfate in Na_2SO_4–H_2SO_4–H_2O solutions. A number of experiments were conducted to study the effect of sodium sulfate concentration, sulfuric acid concentration, and reaction temperature on cerium oxide dissolution and sodium cerium sulfate synthesis in Na_2SO_4–H_2SO_4–H_2O solutions. In addition, the best fitted equation to the experimental data was determined and the optimal conditions for conversion in terms of the three dependent variables above were investigated.

2. Experimental Methods

2.1 Materials

The cerium oxide (CeO_2) powder used in this study was of a chemical grade of 99.9% metal basis (Sigma Aldrich, Ltd.) and the particle size was below 5 µm. The other reagent used was sodium sulfate (Na_2SO_4) from Wako Pure Chemical Industries, Ltd., and was of 99.0% chemical grade.

2.2 Experimental methods and instruments

The experiments on sodium cerium sulfate ($NaCe(SO_4)_2{\cdot}H_2O$) synthesis from cerium oxide in Na_2SO_4–H_2SO_4–H_2O solutions were carried out by using a 500 mL batch glass reactor. Cerium oxide powder at 4 mmol was added to 100 mL of sulfuric acid solutions containing sodium sulfate. The concentration of sodium sulfate ranged from 0.2 to 2.0 mol/dm^3, and the concentration of sulfuric acid from 8 to 14 mol/dm^3. The solution was heated and kept at temperatures of 105, 115, 125 and 135°C under atmospheric pressure. The solution was stirred using magnetic stirrer at 650 rpm.

*Corresponding author, E-mail: hiratou@energy.kyoto-u.ac.jp

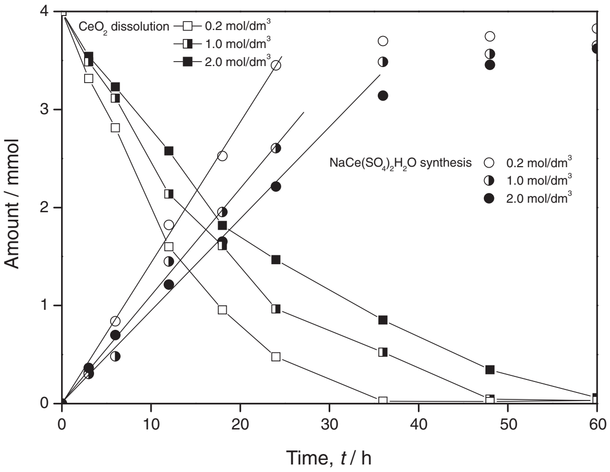

Fig. 1 Effect of sodium sulfate concentration on cerium oxide dissolution and sodium cerium sulfate synthesis kinetics in 0.2–2.0 mol/dm^3 sodium sulfate and 8 mol/dm^3 sulfuric acid solutions at 125°C.

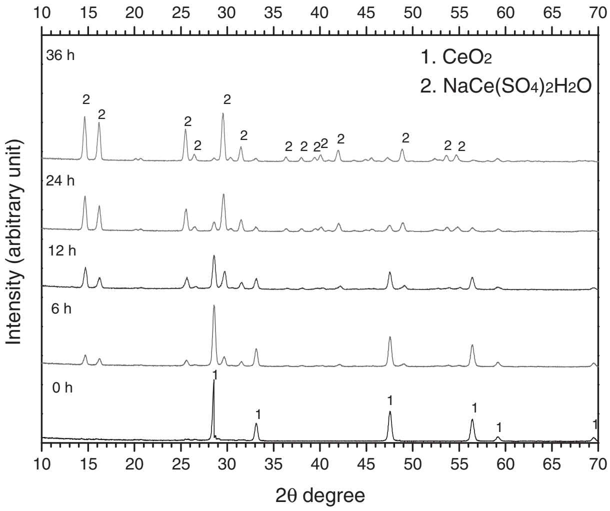

Fig. 2 XRD patterns of the precipitate obtained at different reaction times in 0.2 mol/dm^3 sodium sulfate and 8 mol/dm^3 sulfuric acid solutions at 125°C.

To confirm the conversion kinetics of cerium oxide into sodium cerium sulfate, the samples taken at different reaction times were filtered and measured using an X-ray diffractometer (PANalytical, X'pert PRO) for mineralogical analysis.

For measuring the weight of cerium oxide residue and synthesized sodium cerium sulfate, the precipitate obtained after reaction was filtered from the solution on a 0.5 µm pore size membrane using a pressure filtration unit, and was washed 3 times using ethanol for removal of sulfuric acid. After drying at 45°C for 24 h, the weight (a) of the precipitate consisting of cerium oxide residue and synthesized sodium cerium sulfate was measured using a balance. The precipitate was added into 1 mol/dm^3 sodium hydroxide (NaOH) solution for conversion from sodium cerium sulfate to cerium hydroxide ($Ce(OH)_3$). Then, it was added into 1 mol/dm^3 sulfuric acid solution to dissolve the cerium hydroxide and recover cerium oxide residue. The weight (b) of cerium oxide residue was measured using a balance after drying at 45°C for 24 h. The difference between (a) and (b) determined the weight of synthesized sodium cerium sulfate.

3. Results and Discussion

3.1 Effect of sodium sulfate concentration

The effect of sodium sulfate concentration on the conversion of cerium oxide (CeO_2) into sodium cerium sulfate ($NaCe(SO_4)_2{\cdot}H_2O$) was studied using different sodium sulfate concentrations ranging from 0.2 to 2.0 mol/dm^3. Within these experiment tests, the initial sulfuric acid (H_2SO_4) concentration and reaction temperature were kept constant at 8 mol/dm^3 and 125°C, respectively. The results are given in Fig. 1.

Basically, the amount of cerium oxide decreased monotonically with increasing reaction time, while the amount of synthesized sodium cerium sulfate increased. Namely, the two reactions involving dissolution and synthesis were in synchrony in Na_2SO_4–H_2SO_4–H_2O solutions. The XRD patterns of the precipitates obtained at different reaction times are shown in Fig. 2. The intensity of the diffraction peaks originating from cerium oxide decreased with an increase in reaction time, while that from sodium cerium sulfate increased. This supports the results shown in Fig. 1. These findings indicate that cerium oxide can be converted into sodium cerium sulfate in Na_2SO_4–H_2SO_4–H_2O solutions.

As can be seen in Fig. 1, both the dissolution rate of cerium oxide and the synthesis rate of sodium cerium sulfate were decreased with increasing sodium sulfate concentration. This suggests that the excess of sodium sulfate suppresses the dissolution of cerium oxide. The explanation for this behavior concerns the two chemical reactions given by $H_2SO_4 \rightarrow (a)H^+ + HSO_4^-$ and $Na_2SO_4 \rightarrow 2Na^+ + (b)SO_4^{2-}$ wherein cerium oxide dissolution was suppressed in response to a lowered hydrogen ion concentration caused by the occurrence of $(a)H^+ + (b)SO_4^{2-} \rightarrow HSO_4^-$ with increasing sodium sulfate concentration. Thus the decreasing dissolution rate leads to a decrease of synthesis rate of sodium cerium sulfate; in other words, sodium sulfate concentration does not affect the synthesis rate directly. In addition, the maximum sodium cerium sulfate synthesis yield was 91% under the following conditions: reaction temperature, 125°C; H_2SO_4 concentration, 8 mol/dm^3; and Na_2SO_4 concentration, 0.2 mol/dm^3.

3.2 Effect of sulfuric acid concentration

The effect of sulfuric acid concentration on dissolution and synthesis kinetics at different reaction times is shown in Fig. 3 for 1.0 mol/dm^3 sodium sulfate concentration and sulfuric acid concentrations ranging from 8 to 14 mol/dm^3 at a constant temperature of 125°C. The dissolution rate increased with increasing sulfuric acid concentration, while the synthesis rate decreased. Changing sulfuric acid concentration affects the yield of sodium cerium sulfate according to dissolution and synthesis rates. With 8 mol/dm^3 sulfuric acid concentration, 91% yield of sodium cerium sulfate was obtained after 60 h reaction time, whereas 14 mol/dm^3 acid concentration led to a drop below 10% yield at the same reaction time.

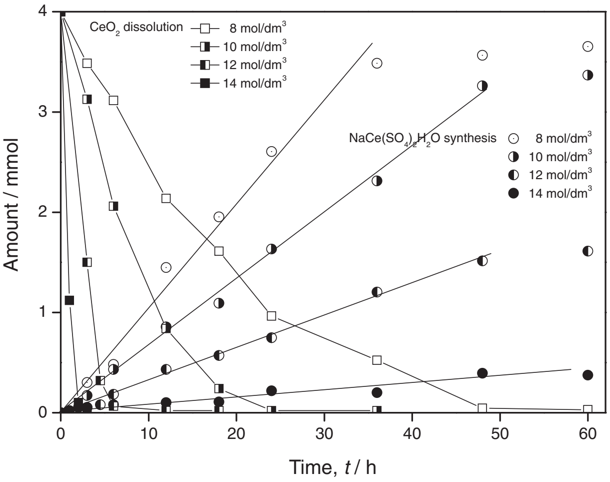

Fig. 3 Effect of sulfuric acid concentration on cerium oxide dissolution and sodium cerium sulfate synthesis kinetics in 1.0 mol/dm^3 sodium sulfate and 8–14 mol/dm^3 sulfuric acid solutions at 125°C.

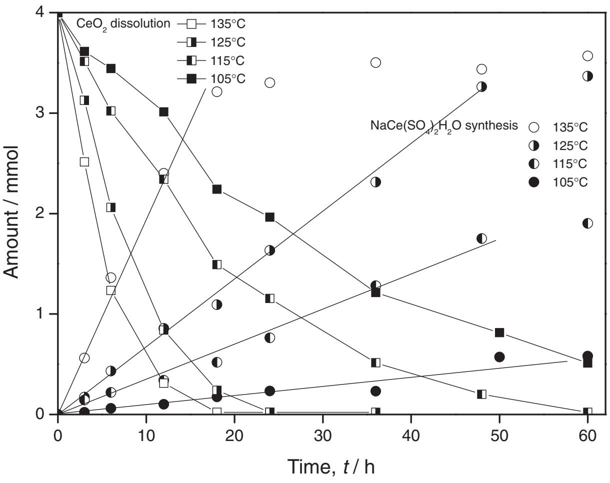

Fig. 4 Effect of reaction temperature on cerium oxide dissolution and sodium cerium sulfate synthesis kinetics in 1.0 mol/dm^3 sodium sulfate and 10 mol/dm^3 sulfuric acid solutions at 105–135°C.

3.3 Effect of reaction temperature

Figure 4 presents the effect of temperature on the reaction rate against time for constant 1.0 mol/dm^3 sodium sulfate and 8 mol/dm^3 sulfuric acid concentrations at different temperatures ranging from 105 to 135°C. Both the dissolution rate of cerium oxide and the synthesis rate of sodium cerium sulfate increased with increasing reaction temperature. Especially the temperature increase from 125 to 135°C strongly improved the synthesis rate: the yield of sodium cerium sulfate that stood at 27% in Na_2SO_4–H_2SO_4–H_2O solutions at 125°C increased to 80% at 135°C.

3.4 Conversion kinetics

The conversion of cerium oxide into sodium cerium sulfate in Na_2SO_4–H_2SO_4–H_2O solutions is supposed to include chemical reactions as follows.

Dissolution of cerium oxide with sulfuric acid solutions at atmospheric pressure can be ascribed as follows:

$$CeO_2 + 4H^+ \rightarrow Ce^{4+} + 2H_2O \quad (1)$$

$$Ce^{4+} + 1/2H_2O \rightarrow Ce^{3+} + H^+ + 1/4O_2. \quad (2)$$

The rate of a reaction between a solid and a fluid can be expressed according to the heterogeneous reaction methods. The fluid-solid heterogeneous reaction process may involve some individual steps such as film diffusion, surface chemical reaction and product layer diffusion controls. Assuming that the reaction rate of cerium oxide dissolution was controlled by the chemical reaction, the data were analyzed using a shrinking-core model as follows:

$$1 - (1 - X_t)^{1/3} = k_1 t, \quad (3)$$

where k_1 is the reaction rate constant (h^{-1}) of cerium oxide dissolution and X_t is the dissolved fraction at time t.

In addition, the dissolution is immediately followed by the synthesis of sodium cerium sulfate as follows:

$$Ce^{3+} + 2Na_2SO_4 + H_2O \rightarrow NaCe(SO_4)_2{\cdot}H_2O + 3Na^+. \quad (4)$$

As shown in Figs. 1, 3 and 4, the amount of synthesized $NaCe(SO_4)_2{\cdot}H_2O$ increased lineally with reaction time. Thus, the synthesis rate of $NaCe(SO_4)_2{\cdot}H_2O$, R_{syn}, can be expressed in terms of rate constant k_2 and time t:

$$R_{syn} = k_2 t. \quad (5)$$

The rate constants k_1 and k_2 vary with experimental conditions such as reaction temperature, sodium sulfate concentration, and sulfuric acid concentration. When cerium oxide is converted into sodium cerium sulfate in Na_2SO_4–H_2SO_4–H_2O solutions, the rate constant, considered as the function of reaction temperature, sodium sulfate concentration, and sulfuric acid concentration, can be expressed by the following equation:

$$k_1 \text{ and } k_2 = k_0' e^{-Ea/RT} N^m C^n, \quad (6)$$

where Ea is the activation energy (kJ/mol); R, the ideal gas constant, 8.314×10^{-3} (kJ/mol K); T, the reaction temperature (K); k_0', pre-exponential factor; N and m, sodium sulfate concentration (mol/dm^3) and a constant; and C and n, sulfuric acid concentration (mol/dm^3) and a constant.

Linear regressions in Figs. 1, 3, 4, 5, 6 and 7 were used to calculate k_1 and k_2 values from the slopes. The dependence of the reaction rate constants on the sodium sulfate concentration was determined from the slopes in Figs. 1 and 5. Figure 8 shows a plot of $\ln k_1$ and $\ln k_2$ versus $\ln N$; from this plot, the kinetic constants, m, of dissolution and synthesis were calculated to be −0.3 and −0.2, respectively. As mentioned above, the sodium sulfate concentration has very little effect on both dissolution and synthesis rates.

The linear regressions in Figs. 3 and 6 were also used to calculate the reaction rate constants for various sulfuric acid concentrations in the conversion of cerium oxide into sodium cerium sulfate; the plots of $\ln k_1$ and $\ln k_2$ versus $\ln C$ in Fig. 9 provide the kinetic constants, n, of dissolution and synthesis, which are 6.5 and −4.3, respectively.

In addition, the slopes of the experimental data in Figs. 4 and 7 were used to determine the reaction rate constants for various temperatures in both the dissolution and the synthesis stages; these data were used for Arrhenius plots, as shown in Fig. 10. The calculated values of the activation energies were

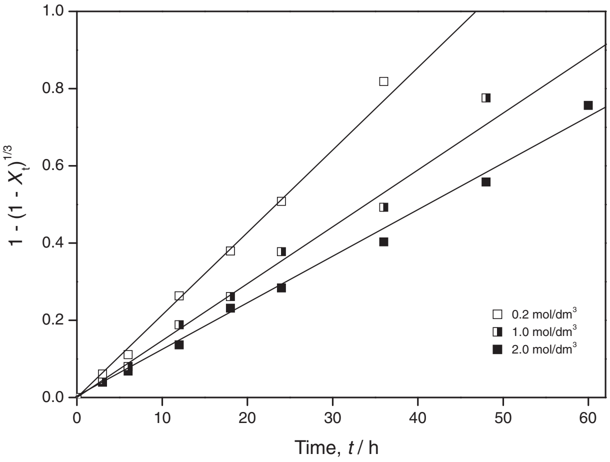

Fig. 5 Plots of $1-(1-X_t)^{1/3}$ versus reaction time for different sodium sulfate concentrations.

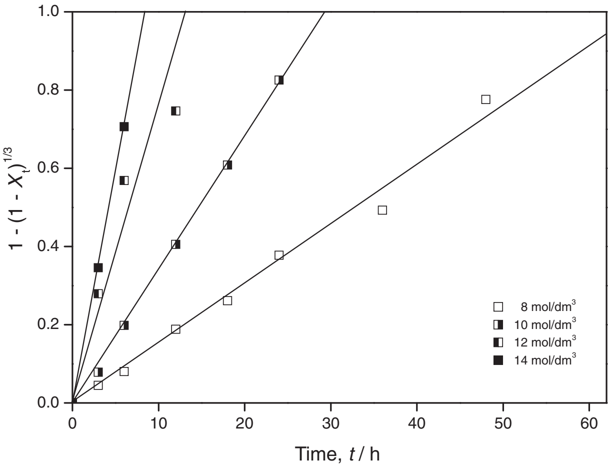

Fig. 6 Plots of $1-(1-X_t)^{1/3}$ versus reaction time for different sulfuric acid concentrations.

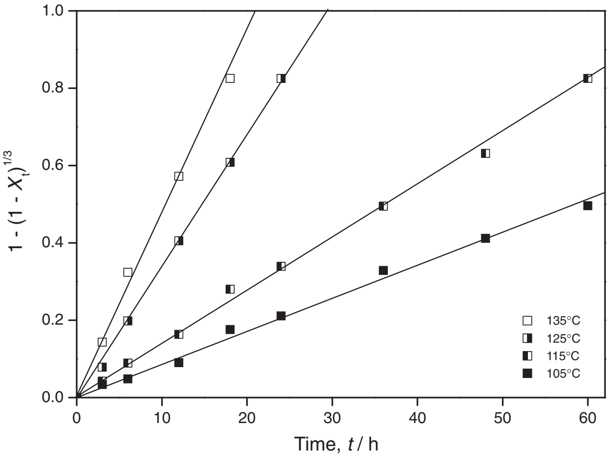

Fig. 7 Plots of $1-(1-X_t)^{1/3}$ versus reaction time for different reaction temperatures.

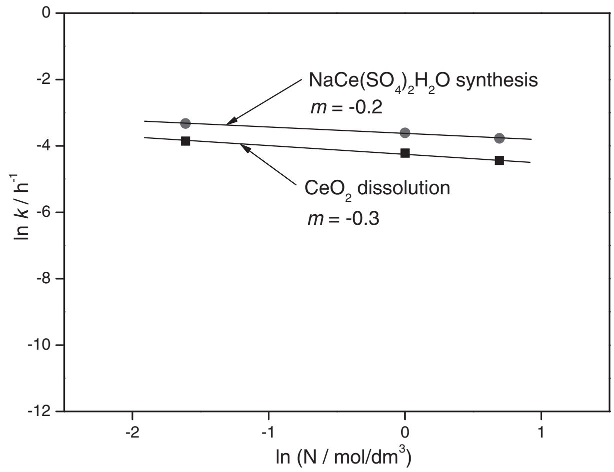

Fig. 8 Effect of sodium sulfate concentration on the dissolution and synthesis rate constants.

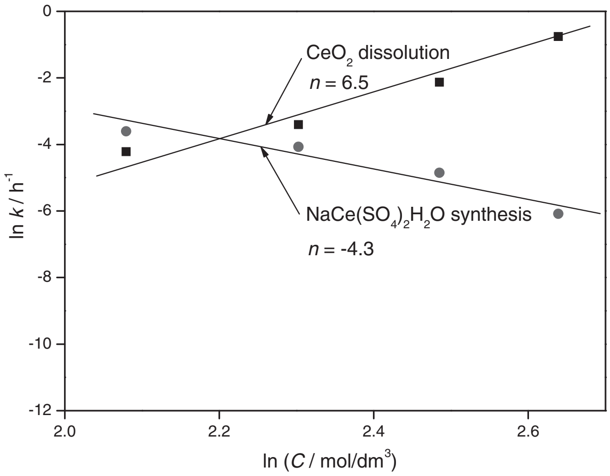

Fig. 9 Effect of sulfuric acid concentration on the dissolution and synthesis rate constants.

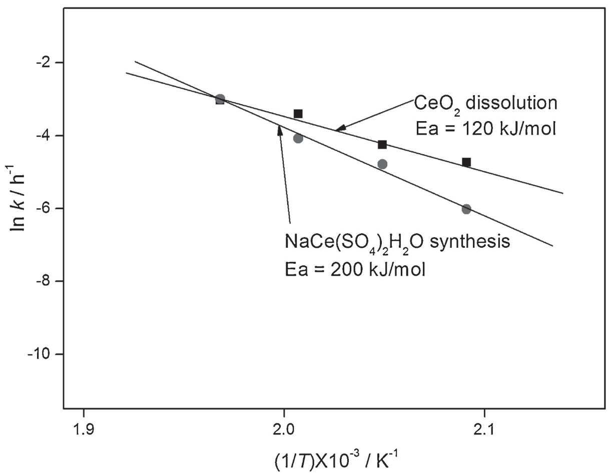

Fig. 10 Effect of reaction temperature on the dissolution and synthesis rate constants.

120 kJ/mol for the cerium oxide dissolution and 200 kJ/mol for sodium cerium sulfate synthesis.

Thus, for the conversion of cerium oxide into sodium cerium sulfate in Na_2SO_4–H_2SO_4–H_2O solutions, the kinetics equations were obtained as follows:

$$k_1 = 1.23 \times 10^8 e^{-14540/T} N^{-0.3} C^{6.5} \quad (7)$$

$$k_2 = 2.27 \times 10^{28} e^{-23790/T} N^{-0.2} C^{-4.3}. \quad (8)$$

4. Conclusion

The conversion kinetics of cerium oxide (CeO_2) into sodium cerium sulfate ($NaCe(SO_4)_2 \cdot H_2O$) in Na_2SO_4–H_2SO_4–H_2O solutions was investigated and the results were as follows.

The conversion process has chemical reactions as follows:

$$CeO_2 + 4H^+ \rightarrow Ce^{4+} + 2H_2O$$
$$Ce^{4+} + 1/2H_2O \rightarrow Ce^{3+} + H^+ + 1/4O_2$$
$$Ce^{3+} + 2Na_2SO_4 + H_2O \rightarrow NaCe(SO_4)_2 \cdot H_2O + 3Na^+.$$

Cerium oxide dissolved in high-acid-concentration solutions, and the dissolution was immediately followed by sodium cerium sulfate synthesis.

In the conversion process, sodium sulfate (Na_2SO_4) concentration, sulfuric acid (H_2SO_4) concentration and reaction temperature were found to be the factors that affected the dissolution and the synthesis rate. For this reason, the result showed that an excess of sodium sulfate suppresses cerium oxide dissolution and leads to a decrease in the rate of sodium cerium sulfate synthesis. In addition, although the increase in sulfuric acid concentration increased the cerium oxide dissolution rate, it decreased the synthesis rate. Both cerium oxide dissolution and sodium cerium oxide synthesis rates, however, increased with an increasing reaction temperature.

Conditions under which the maximum sodium cerium sulfate synthesis yield was obtained were determined as follows: reaction temperature, 125°C; sulfuric acid concentration, 8 mol/dm^3; sodium sulfate concentration, 0.2 mol/dm^3; and reaction time, 48 h, with which 91% yield was obtained. However when the reaction temperature was adjusted to 135°C, the reaction time could be shortened to 18 h even though the sulfuric acid concentration was raised to 10 mol/dm^3.

The calculated values of the activation energies in dissolution and synthesis were 120 and 200 kJ/mol, respectively. In addition, the rate constants can be expressed as a function of sodium sulfate concentration and sulfuric acid concentration as well as reaction temperature as $k_1 = 1.23 \times 10^8 e^{-14540/T} N^{-0.3} C^{6.5}$ and $k_2 = 2.27 \times 10^{28} e^{-23790/T} N^{-0.2} C^{-4.3}$ for cerium oxide dissolution and sodium cerium sulfate synthesis, respectively.

Acknowledgments

The authors are grateful for the support of the Ministry of Education, Culture, Sports, Science and Technology of Japan via “Energy Science in the Age of Global Warming” of the Global Center of Excellence (G-COE) program (J-051).

REFERENCES

1) R. Sabia, H. J. Stevens and F. R. Varner: J. Non-Crystalline Solids **249** (1999) 123–130.
2) N. S. Ong and V. C. Venkatesh: Mater. Process. Technol. **83** (1998) 261–266.
3) V. D. Kosynkin, A. A. Arzgatkina, E. N. Ivanow, M. G. Chtoutsa, A. I. Grabko, A. V. Kardapolow and N. A. Sysina: J. Alloy. Compd. **303–304** (2000) 421–425.
4) T. Hoshino, Y. Kurata, Y. Terasaki and K. Susa: J. Non-Crystalline Solids **283** (2001) 129–136.
5) X. Tao and P. Huiqing: J. Rare Earths **27** (2009) 1096–1102.
6) S. Chong, D. Holmstrom, Q. Li and T. Ouyang: VATTEN **65** (2009) 193–200.
7) H. S. Yoon, H. C. Eom and J. S. Kim: J. Korean Inst. Resources Recycl. **14** (2005) 3–9.
8) H. S. Yoon, C. J. Kim, D. S. Kim, J. Y. Lee, S. W. Cho and J. S. Kim: J. Korean Inst. Resources Recycl. **12** (2003) 10–15.
9) T. Ozaki, K. I. Machida and G. Y. Adachi: Metall. Mater. Trans. B **30** (1999) 45–51.
10) A. C. Blackburn and R. E. Gerkin: Acta Cryst. C **51** (1995) 2215–2218.
11) E. P. Lokshin, O. A. Tareeva, K. G. Ivlew and T. G. Kashulina: Russ. J. Appl. Chem. **78** (2005) 1058–1063.
12) R. D. Abreu and C. A. Morais: Miner. Eng. **23** (2010) 536–540.
13) M. Kul, Y. Topkaya and I. Karakaya: Hydrometallurgy **93** (2008) 129–135.
14) D. A. Bertuol, A. M. Bernardes, H. Holeczed and H. J. Fetzer: Acta Metall. Slovaca **12** (2006) 13–19.